



ELSEVIER

Available online at [www.sciencedirect.com](http://www.sciencedirect.com)

SCIENCE @ DIRECT®

Nuclear Instruments and Methods in Physics Research A 505 (2003) 174–177

**NUCLEAR  
INSTRUMENTS  
& METHODS  
IN PHYSICS  
RESEARCH**  
Section A[www.elsevier.com/locate/nima](http://www.elsevier.com/locate/nima)

# Performance of a $6 \times 6$ segmented germanium detector for $\gamma$ -ray tracking

J.J. Valiente-Dobón<sup>a,\*</sup>, C.J. Pearson<sup>a</sup>, P.H. Regan<sup>a</sup>, P.J. Sellin<sup>a</sup>,  
W. Gelletly<sup>a</sup>, E. Morton<sup>a</sup>, A. Boston<sup>b</sup>, M. Descovich<sup>b</sup>, P.J. Nolan<sup>b</sup>,  
J. Simpson<sup>c</sup>, I. Lazarus<sup>c</sup>, D. Warner<sup>c</sup>

<sup>a</sup>Department of Physics, University of Surrey, Guildford, GU2 7XH, UK

<sup>b</sup>Department of Physics, University of Liverpool, Liverpool, L69 3BX, UK

<sup>c</sup>CLRC, Daresbury Laboratory, Warrington, WA4 4AD, UK

## Abstract

A 36 fold segmented germanium coaxial detector has been supplied by EURISYS MESURES. The outer contact is segmented both radially and longitudinally. The signals from the fast preamplifiers have been digitised by 12 bit, 40 MHz ADCs. In this article we report preliminary results obtained using this detector and their relevance for future germanium  $\gamma$ -ray tracking arrays.

© 2003 Elsevier Science B.V. All rights reserved.

*Keywords:* Gamma-ray tracking; Segmented germanium detectors

## 1. Introduction

Germanium detectors have attained great importance in  $\gamma$ -ray spectroscopy. They offer both good energy resolution and acceptable efficiency for energies between 10 keV and 10 MeV. Arrays of germanium spectrometers [1,2] have been developed as an important tool for the study of the complex structure of atomic nuclei. However, the capabilities of these arrays are limited by (i) the total photo-peak efficiency with values around 10% for EUROBALL [12] and GAMMA-SPHERE [1], and ranging up to 20% in the case of EXOGAM [3], (ii) the Peak to Compton background ratio and (iii) the limited Doppler

shift correction due to the finite opening angle of the individual detectors. The rapid development of facilities providing beams of radioactive ions such as SPIRAL, ISAC, RIA, EURISOL and SIS/FRS will place new demands on such detectors. They will require an improvement in efficiency, Peak to Total ratio, better position resolution of the first interaction for Doppler shift correction and higher count rate capabilities. In this article we describe the first results obtained using a 36 fold segmented germanium detector, ultimately for use in  $\gamma$ -ray tracking.

## 2. Description of the $6 \times 6$ segmented detector and the data acquisition

A prototype highly segmented, coaxial hyper-pure n-type germanium detector with external diameter 60 mm and length 90 mm has been

\*Corresponding author.

E-mail address: [j.valiente-dobon@surrey.ac.uk](mailto:j.valiente-dobon@surrey.ac.uk)  
(J.J. Valiente-Dobón).

constructed by EURISYS MESURES (EGC 60–90 SEG36). The outer, p<sup>+</sup> ion-implanted, contact of the crystal is segmented into six segments in both the longitudinal and radial directions and the thickness of each segment is 15 mm (see Fig. 1).

The inner contact is n<sup>+</sup> lithium diffused. This contact is not segmented and can be used to provide a total energy signal for the full crystal. This contact is positive polarized at 3500 V. The preamplifiers, with room temperature FETs, are placed immediately after the crystal and are based on a fast risetime (29 ns), University of Cologne design.

In each event the signals from the 36 segments are digitised using six cM62 boards, provided by OMNIBUS, where each one comprises six channels with a single Digital Signal Processor (DSP). Fig. 2 shows a detailed schematic view of the electronics. The signal from the charge preamplifiers are fed into a Low Distortion Amplifier, then to a 12 bit, 40 MHz flash ADC which digitises the signal. The trigger for the ADCs is given by the inner contact of the detector.

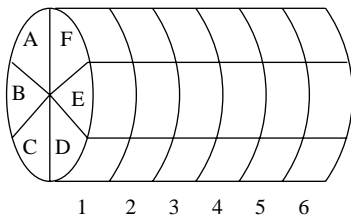


Fig. 1. Schematic labelled view of the outer contact segmentation.

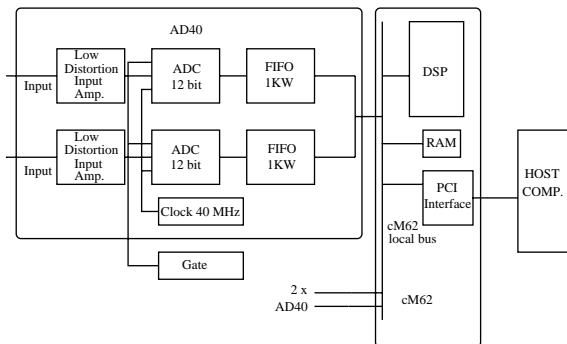


Fig. 2. Diagram of the electronics used for pulse processing, single cM62 module.

### 3. Performance of the 6 × 6 segmented detector

Fig. 3 shows the energy resolution performance for the 36 segments. An external spectroscopic amplifier with a 6 μs shaping time was used to measure the FWHM at 1332 keV (<sup>60</sup>Co), and at 122 keV (<sup>57</sup>Co). The energy resolution of the full crystal at 122 and 1332 keV was measured to be 3.60 and 4.10 keV, respectively. No cross-talk between the segments was found.

The coaxial segments present a better resolution than the front segments. This fact can be explained by the smaller surface that the coaxial segments present to the aluminium can, giving a smaller capacitance, thus decreasing the noise contribution [4].

Fig. 4 shows the distribution of the risetime (T10%–T90%) calculated from the digitised signal for γ-ray energies of 1332 keV for two different longitudinal slices. Inspection of these plots shows that the risetime distribution from the front slice is broader and the peak value (~150 ns) is higher than in slice three (~125 ns). This can be explained if we recall that the crystal has closed-ended coaxial geometry. In the case of the front edge of the crystal there are areas in the edges of the crystal where the electric field is weaker, thus the collection of the electrons and holes takes longer increasing the risetime. Moreover it will contribute to broadening the risetime distribution.

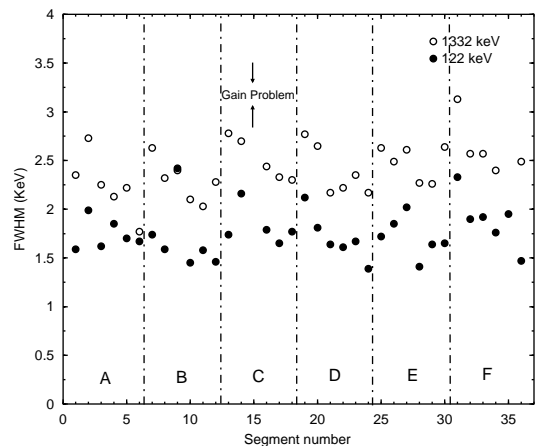


Fig. 3. Energy resolution for all the working segments, obtained using a 6 μs shaping time amplifier.

### 4. Signal processing

Ramo’s theorem [5] gives a theoretical description of instantaneous signal formation due to the motion of the charge carriers in a semiconductor.

$$i(t) = q\mathbf{E}_w(\mathbf{r})\mathbf{v}(t) \tag{1}$$

where  $q$  is the charge produced in the event,  $\mathbf{v}(t)$  is the velocity of the moving charge and  $\mathbf{E}_w$  is defined as the *weighting field*. The weighting field is a measure of electrostatic coupling between the moving charge and the sensing electrode. This theorem describes both the net charge and transient signals as can be seen in the simulations presented in Ref. [6].

The position resolution given by the segmentation of the crystal can be improved by analysing the net and mirror charge signals described by Ramo’s theorem. The *radial position* of the main interaction is determined by the risetime of the pulse, which is given by the collection time of the electrons and holes.

As pointed out in Ref. [9] the poorest position resolution is where the electron and hole travel times are equal and the signal risetime is a minimum.

The *azimuthal position* is determined from the mirror charges induced in the neighbouring segments. The mirror charge signal has a maximum while electrons and holes are drifting in the segment where the interaction occurred and goes to zero when they have been collected. The amplitude of the mirror charges depends on the distance to the neighbouring segment of the main interaction and the radial position. The mirror charge is negative if the main interaction occurs close to the inner contact, the pulse is mainly induced by drifting holes and is positive if the interaction happens close to the outer contact, where the signal is mainly induced by drifting electrons [6].

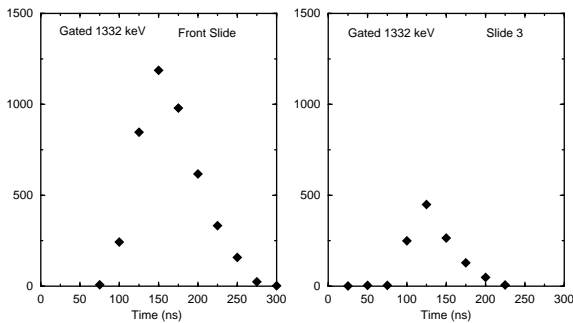


Fig. 4. Risetime distributions, for 1332 keV  $\gamma$ -rays, for the front slice (slice 1) and slice 3.

Fig. 5 shows digitised signals from the  $6 \times 6$  Eurysis prototype. Each signal has 256 samples (one each 25 ns) covering around  $5 \mu\text{s}$ . Both events show a net charge in segment E3. Event I shows a  $\gamma$ -ray interaction which deposited approximately

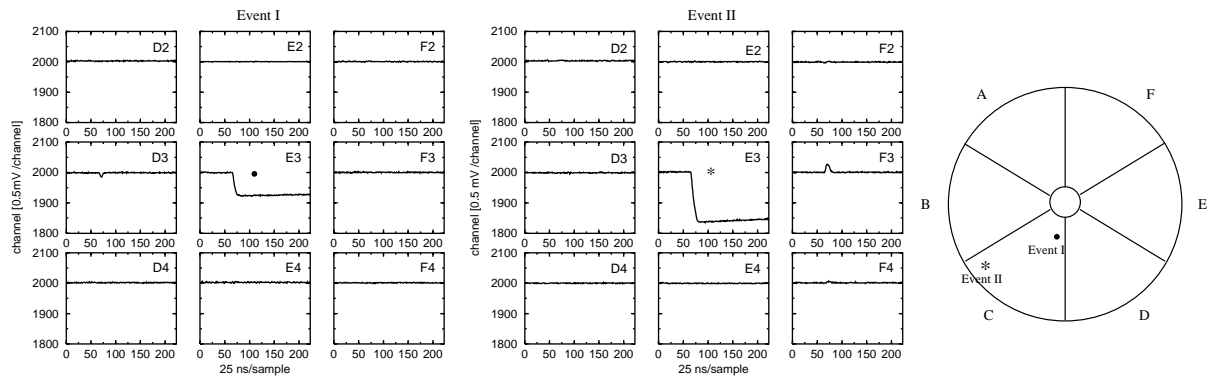


Fig. 5. Digitised signals using the electronics described earlier (see text). It shows, for two different events, the net charge in segment E3 in both cases (middle plot) and mirror charge signals in the neighbouring segments.

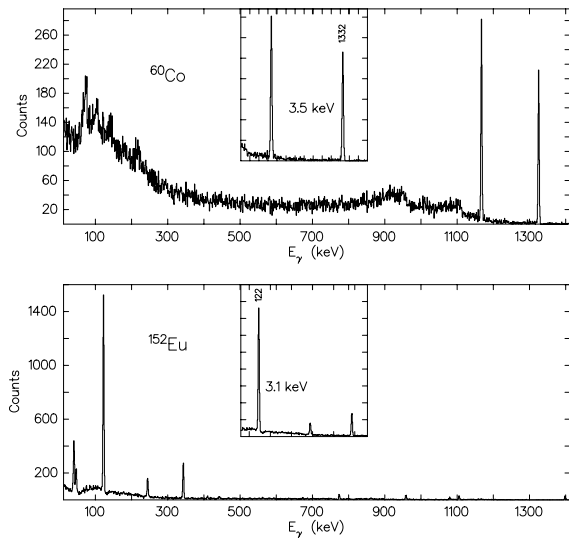


Fig. 6. Performance of the MWD method for  $^{60}\text{Co}$  and  $^{152}\text{Eu}$  sources for segment B1 (front edge).

200 keV and it manifests a negative mirror charge in D3, i.e., the main interaction occurred in segment E3 close to the inner contact nearby D3. Event II shows an energy deposition of approximately 430 keV and a positive mirror charge in F3, i.e., the main interaction occurred in segment E3 close to the outer contact nearby F3. These examples show crudely that it is possible to say where the interaction happened, looking at the hit and the neighbouring segments. Approaches to defining the interaction position accurately have been based on methods of artificial intelligence, genetic algorithms (GA), artificial neural networks (ANN) [7] and Discrete Wavelet Transform (DWT) [8].

The interaction energy provides vital information for tracking purposes [10]. The Moving Window Deconvolution method (MWD) [11] was used to obtain the deposited energy with high resolution from the digitised signals. Fig. 6 shows the performance of the MWD method for  $^{60}\text{Co}$  and  $^{152}\text{Eu}$  sources. A FWHM of 3.5 and 3.1 keV for the energies 1.332 MeV and 122 keV respectively was found for segment B1 (front edge), compared with 2.7 and 1.7 keV obtained using a 6  $\mu\text{s}$  shaping time amplifier.

### Acknowledgements

This research project is funded by the EPSRC (UK).

### References

- [1] P.J. Nolan, F.A. Beck, D.B. Fossan, *Annu. Rev. Nucl. Part. Sci.* 45 (1994) 561.
- [2] C.W. Beausang, J. Simpson, *J. Phys. G: Nucl. Part. Phys.* 22 (1996) 527.
- [3] J. Simpson, et al., *Heavy Ion Physics* 11 (2000) 159.
- [4] K. Vetter, et al., *Nucl. Instr. and Meth. A* 452 (2000) 105.
- [5] V. Radeka, *Ann. Rev. Nucl. Part. Sci.* 38 (1988) 217.
- [6] Th. Kröll, D. Bazzacco, *Nucl. Instr. and Meth. A* 463 (2001) 227.
- [7] Th. Kröll, et al., *LNL Annual Report*, 1998.
- [8] L. Mihailescu, *Doctoral Thesis*, Forschungszentrum Jülich, 2000.
- [9] J. Blair, et al., *Nucl. Instr. and Meth. A* 422 (1999) 331.
- [10] C.J. Pearson, et al., *IEEE Trans. Nucl. Sci.* NS-49 (3) (2002) 1209.
- [11] A. Georgiev, W. Gast, *IEEE Trans. Nucl. Sci.* NS-40 (1993) 770.
- [12] J. Simpson, et al., *Z. Phys. A* 358 (1997) 139.